Earthquake Geotechnical Engineering for Protection and Development of Environment and Constructions – Silvestri & Moraci (Eds)
© 2019 Associazione Geotecnica Italiana, Rome, Italy, ISBN 978-0-367-14328-2

Modeling reinforcing effects of ground improvement in mitigating seismic settlement

J.R. Gingery
Hayward Baker, Inc., San Diego, California, USA

ABSTRACT: Liquefaction related building foundation settlement occurs by some combination of various mechanisms: consolidation and resedimentation (collectively, volumetric settlements), ejecta, and shear distortion. Ground improvement has long been utilized to mitigate liquefaction hazards for building foundations and has generally resulted in good performance in earthquakes. Arrays of stone column ground improvement counteract liquefaction through three potential mechanism: densification, drainage and reinforcement. This paper presents a numerical study examining the effectiveness of stone columns to mitigate volumetric settlements in liquefiable soils by the reinforcement mechanism. An axisymmetric model is adopted based on periodic boundary concepts to represent a distributed array of stone columns. The model simulates only the post-shaking porewater pressure dissipation and settlement part of the problem. A constitutive model is proposed as an extension of the elastic perfectly plastic model in which the elastic parameters are varied nonlinearly with effective stress during excess porewater dissipation such that target volumetric strains are achieved. The numerical model is validated against centrifuge test data from the literature. The results provide insight into the mechanisms at work in ground improvement reinforcement with respect to mitigation of post-liquefaction volumetric settlements.

1 INTRODUCTION AND BACKGROUND

The settlement of structures as a result of liquefaction phenomena can result in significant damage. For example, settlements of buildings in the Canterbury earthquake sequence resulted in structural damage and tilting of buildings to the extent that many structures were considered unusable and were subsequently demolished (Bray et al. 2014). Bray et al. (2017) have identified the various mechanisms of liquefaction-related settlement: consolidation and resedimentation (herein, collectively referred to as volumetric settlements), ejecta and shear distortion. Researchers have developed techniques for estimating reconsolidation settlements which have been in use by practitioners for many years (e.g., Tokimatsu and Seed 1987, Ishihara and Yoshimini 1992). More recently, analysis methods have been developed for the engineering estimation of building settlement caused by shear loading and liquefaction ejecta (Bray and Macedo 2017, Bullock et al. 2018).

Various forms of ground improvement can be used to mitigate liquefaction hazards (Mitchell et al. 1998) and performance of ground improvement in strong earthquakes has generally been good (Hausler and Sitar 2001). Vibro-replacement stone columns (stone columns) are a method in which a vibratory probe is advanced into the ground using vibration and (if necessary) water jetting and compressed air. Crushed rock is introduced to the bottom of the column and the probe is cyclically withdrawn and advanced while vibrating to densify the stone and displace it laterally into the ground. The combination of vibration and lateral displacement densifies the surrounding ground. In liquefaction mitigation applications the columns are typically constructed in continuous triangular or square arrays throughout the footprint of the building.

Stone columns act through several mechanisms to increase soil resistance to liquefaction and improve seismic building performance. These mechanisms include densification of the

in-situ soils, enhanced drainage, shear reinforcement, and strengthening and stiffing of the composite ground (Kirsch and Kirsch 2010). For cases where the in-situ densification is sufficient to preclude liquefaction triggering, liquefaction-related settlements are essentially eliminated. In cases where in-situ soils are too loose or too fine grained to be densified enough to preclude liquefaction, the drainage and reinforcing effects of stone columns act to mitigate liquefaction related settlements. The axial reinforcing effects of stone columns in reducing static settlements from surface loading have been studied and simplified analysis methods are available for practitioners (Priebe 1995, Sehn and Blackburn 2008). But reduction of liquefaction-related settlement by stone column reinforcement is not as well understood and simplified analysis methods are not currently available. More advanced dynamic numerical modeling methods can be used, but many such models underpredict reconsolidation strains and the effort and rigor involved with such methods may not be practical for routine projects.

This paper focuses on stone column reinforcement effects in reducing post-liquefaction reconsolidation settlements. In North American design practice it is common to estimate post-ground improvement reconsolidation settlements using free field techniques (e.g., Tokimatsu and Seed 1987 or Ishihara and Yoshimine 1992) applied to Standard Penetration Test (SPT) or Cone Penetration Test (CPT) data taken at the mid-point between adjacent stone columns. Representing liquefaction settlements in this way is potentially overly conservative in two ways: 1) the mid-point between stone columns has been subjected to the least compactive energy and is likely the least dense zone of the in-situ soil; and 2) use of free field techniques does not account for the axial reinforcing effect of the stone columns. The first aspect can be addressed by performing SPT or CPT testing at points other than the mid-point and taking averages. This paper addresses the second aspect – the potential for axial reinforcement by stone columns to result in settlement less than free field values.

In this paper the axial reinforcing effect is investigated using a numerical modeling approach. A constitutive model is developed to represent post-liquefaction reconsolidation behavior. The model is validated against centrifuge test results and the mechanisms at work in the stone column reinforcement area explored.

2 LITERATURE REVIEW

Constitutive models that capture important aspects of liquefaction behavior such as contraction, dilation, porewater pressure generation, phase transformation and cyclic mobility have been developed and are available for use in finite element and finite difference software (e.g., Beaty and Byrne 2011, Boulanger and Ziotopoulou 2015, Khosravifar et al. 2018,). When appropriately calibrated, such models have been shown to provide reasonable predictions of liquefaction triggering and shear related deformations. However, many such models are formulated such that post-liquefaction settlements are significantly underestimated.

Ziotopoulou and Boulanger (2013) amended the PM4Sand model with a post-shaking reconsolidation feature that scaled the elastic moduli according to a shear strain accumulation damage parameter in order to produce reconsolidation settlements approximating lab data from Ishihara and Yoshimine (1992). This model was considered for use in this study but ultimately was not selected since it could not be applied to the axisymmetric modeling configuration that was used.

3 MODEL DEVELOPMENT

3.1 *Constitutive model*

A simple constitutive model was developed in FLAC (Itasca Consulting Group 2016) for the purpose of representing the post-liquefaction reconsolidation behavior of sand. The model was formulated with the goal of capturing behavior important in the reconsolidation and columnar reinforcement mechanics. Specifically, the model should: 1) produce a specified target volumetric strain in a free field condition; 2) represent the softened and weakened state of the

liquefied soil and the gradual re-stiffening and strengthening that occurs during porewater pressure dissipation and reconsolidation; and 3) reestablish the initial strength and stiffness upon dissipation of porewater pressure. With these desirable behaviors in mind, an effective stress-based model was developed that varies the constrained modulus with effective stress according the following equation:

$$M = M_{liq} + (M_0 - M_{liq})\left(\frac{\sigma'_m - (1 - r_{u,\max})\sigma'_{m0}}{r_{u,\max} \cdot \sigma'_{m0}}\right)^n \quad (1)$$

where σ'_{m0} is the initial mean effective stress, σ'_m is the mean effective stress during liquefaction and reconsolidation, M_0 is the initial (pre-liquefaction) constrained modulus, $r_{u,max}$ is the maximum excess porewater pressure ratio when the soil is liquefied ($r_{u,max} = \Delta u/\sigma'_{v0}$, where Δu is the excess porewater pressure), M_{liq} is the liquefied constrained modulus calculated as $M_{liq} = (1 - r_{u,max})M_0$, and exponent n is a calibration constant. Using elasticity theory the constrained modulus is related to the shear modulus (G), bulk modulus (K) and the Poisson's ratio (υ) by:

$$G = \frac{M(1 - 2\upsilon)}{2(1 - \upsilon)} \quad (2)$$

$$K = \frac{M(1 + \upsilon)}{3(1 - \upsilon)} \quad (3)$$

All of the elastic parameters listed above are effective stress-based. During liquefaction and reconsolidation the shear and bulk moduli are continuously updated using Eqn's 2 and 3 with a constant Poisson's ratio and the constrained modulus according to Eqn. 1. Under one-dimensional conditions post liquefaction reconsolidation strains are calculated by the following integral:

$$\varepsilon_{vol} = \int_{\sigma'_{v0}}^{\sigma'_{v,liq}} \frac{1}{M} d\sigma'_v \quad (4)$$

where $\sigma'_{v,liq} = (1 - r_{u,max})\sigma'_{v0}$. It is not possible to solve Eqn's 1 and 4 analytically for n, so numerical integration must be performed iteratively to determine n for a given set of target ε_{vol}, $r_{u,max}$, and initial moduli and stresses.

An example of the model performance is shown in Figure 1 for a case where $\varepsilon_{vol} = 3\%$, $\sigma'_{v0} = 0.5$ atm, $K_0 = 0.43$, $r_{u,max} = 0.98$, $\upsilon = 0.3$, and the initial pre-liquefaction shear modulus is 7851

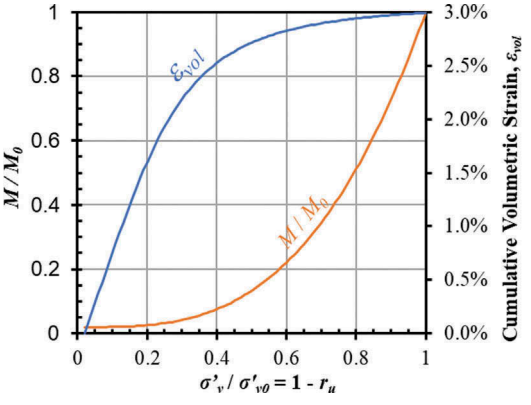

Figure 1. Example of model behavior during porewater pressure dissipation and reconsolidation.

kPa atm. Figure 1 shows the ratio of the constrained modulus to the initial pre-liquefaction constrained modulus (M/M_0) and the cumulative volumetric strain against the excess porewater pressure ratio. The exponent value for this condition is, $n = 3.13$.

It should be noted that the model does not work unconditionally for all combinations of σ'_{v0}, $r_{u,max}$, υ, and G_0, and n. However, typical target volumetric strain values ranging from 1 to 5 percent can generally be achieved with reasonable combinations of these parameters.

3.2 *Numerical implementation*

The constitutive model was implemented in FLAC as a fish function that modifies the elastic moduli used in the Mohr-Coulomb elastic perfectly plastic model. The phases of the modeling are as follows: 1) assign the pre-liquefaction static soil properties and establish equilibrium with the initial pre-liquefaction stresses conditions; 2) incrementally increase the porewater pressure until the desired $r_{u,max}$ is achieved (drainage is not allowed in this phase); 3) establish the drainage boundary conditions and allow groundwater diffusion to occur until the excess porewater pressures are dissipated. The third phase involves solving a coupled fluid-mechanical process in which an increment of fluid diffusion occurs followed by steps to solve for mechanical equilibrium. The elastic moduli are updated at each fluid-mechanical step during the third phase. The diffusion process continues until the excess porewater pressures are completely dissipated.

4 MODEL VALIDATION

4.1 *Adalier et al. (2003) centrifuge tests*

Adalier et al (2003) performed a series of four centrifuge tests to evaluate the effect of stone columns as a liquefaction countermeasure. Model 1 and Model 2 were conducted at a centrifugal acceleration of 50g and consisted of soil placed within a laminar box with prototype dimensions of 23 m long by 12.5 m wide by 7.8 m high. Model 1 consisted only of silt with a relative density of 60% and internal angle of friction (ϕ) of 25 degrees while Model 2 used the same silt with a 9 by 5 array of "stone columns" with diameters of 1.26 m and square spacing of 2.5 m (area replacement ratio of 20%). The stone columns consisted of Nevada No. 120 sand with a friction angle of 37 degrees. The experiments were instrumented with porewater pressure transducers, accelerometers and linear variable differential transformers for measuring surface settlements. Models 3 and 4 were constructed with surficial loading from a footing and were not used in this validation. Shaking was applied at the base of the container as a tapered sinusoidal wave with 20 cycles, a frequency of 1.8 Hz and a peak acceleration of 0.3g.

Profiles of maximum excess porewater pressure ratio achieved in Models 1 and 2 are presented in Figure 2. The data show the entire soil profile in Model 1 liquefied with $r_u = 1$. In

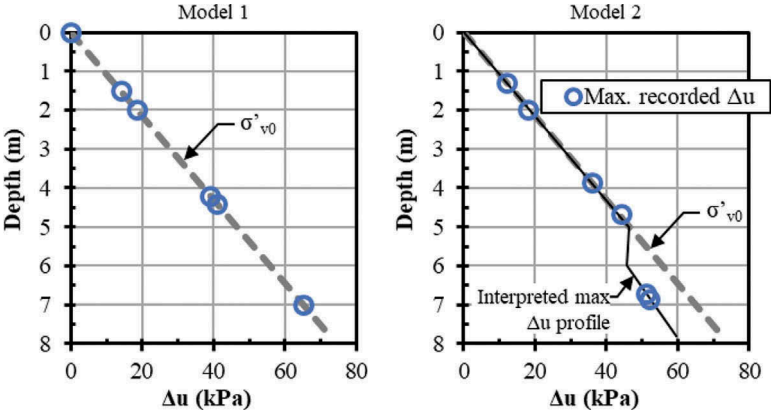

Figure 2. Excess porewater pressure profiles from Adalier et al. (2003) Models 1 and 2.

Model 2 the upper 5.5 meters liquefied with r_u = 1 whereas the lower approximately 2.3 m achieved r_u = 0.82. The reduction in r_u in Model 2 likely occurred due to a combination of stone column drainage and shear reinforcement (Rayamajhi et al. 2016) effects.

In Model 1 representing free field conditions without stone columns, the total liquefaction settlement was 0.1 m corresponding to an average volumetric strain of 1.3 percent. In Model 2 the surface settlement measured at points in the silt between the stone columns was 0.07 m, which represents an overall reduction of 30 percent compared to the free field case.

Some of the reduction of settlement in Model 2 may be attributable to the fact that the lower portions of the model did not fully liquefy as it did in Model 1. Settlement versus depth measurements were not available so volumetric strain versus depth could not be calculated. As part of the present study an estimate was made of the volumetric strain versus depth in Model 2. Using the relationship between r_u and factor of safety against liquefaction (FS_l) from Tokimatsu and Seed (1987), FS_l was estimated to be 1.03 for r_u = 0.82. With FS_l = 1.03 and D_r = 60% the volumetric strain chart of Ishihara and Yoshimine (1992) was used to determine a volumetric strain of 1%. For comparison, with Model 1 a volumetric strain of 1.3% and D_r = 60% produces FS_l = 0.97 with Ishihara and Yoshimine (1992). For equivalent Model 2 free field conditions, the expected settlement is (2.3 m)(0.01) + (5.5 m)(0.013) = 0.095 m, which is more than the observed Model 2 settlement of 0.07 m. This suggests that the reduction in settlement observed in Model 2 compared to Model 1 was from a combination of reduced excess porewater pressures in the lower part of the model and vertical reinforcing effects of the stone columns.

4.2 *Numerical simulation*

Models 1 and 2 were simulated in FLAC with the proposed constitutive model. A unit cell approach was adopted for Model 2 consisting of a single stone column and the surrounding soil. An axisymmetric model was used with the stone column width set to the radius of the stone column and the radius of the model set such that the 20% area replacement ratio was achieved. A finite difference mesh with a nominal dimension of 0.1 m was used. Figure 3 shows the geometry, mesh and boundary conditions for Model 2. The conditions for Model 1 are identical except that there is no stone column and silt occupies the entire model domain.

The unit weight, relative density, strength and hydraulic conductivity values used in the model were based on those reported in Adalier et al. (2003) and are summarized in Table 1.

Stiffness parameters were not reported by Adalier et al. (2003) so the small strain shear modulus was estimated for the silt using the following relationships (Boulanger and Ziotopoulu 2015):

$$G = G_0 p_a \left(\frac{\sigma'_m}{p_a}\right)^{1/2} \tag{5a}$$

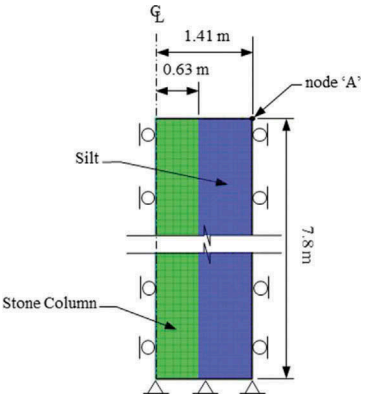

Figure 3. FLAC numerical model geometry, mesh and boundary conditions for Model 2.

Table 1. Summary of soil parameters

Material	γ (kN/m^3)	D_r	ϕ (deg.)	c (kPa)	k (cm/s)
Silt	19.1	60%	25	2	4.3e-4
Stone Column	19.65	n/a	37	0	2.6e-1

$$G_0 = 167\sqrt{(N_1)_{60} + 2.5} \tag{5b}$$

$$D_r = \sqrt{\frac{(N_1)_{60}}{46}} \tag{5c}$$

where σ'_m is the initial mean effective stress and p_a is atmospheric pressure and $(N_1)_{60}$ is the normalized SPT blow count. The normalized low strain shear modulus for the silt (G_0) was calculated to be 728 using Equations 5a and 5b with D_r = 60%. Values of G varying with σ'_m were calculated using Equation 5a and then further reduced by a factor of 0.15 to account for shear modulus reduction that would occur as a result of working shear strain levels. The shear modulus for stone was calculated assuming it was seven times stiffer than the silt (G_r = 7). This value is consistent with typical values used by Rayamajhi et al. (2016). A Poisson's ratio of 0.3 was used for both the silt and stone column materials.

While the value of $r_{u,max}$ obtained in the centrifuge model was essentially 1.0 for liquefied silt, a value of $r_{u,max}$ = 0.96 was used in the numerical model to avoid numerical instability issues associated with a condition of zero effective stress. For both Model 1 and Model 2 the target volumetric strain in the liquefied silt (where $r_{u,max}$ = 1 in Figure 2) was set to 1.3 percent based on the free field volumetric strain observed in centrifuge test results for Model 1. In the lower 2.3 m of silt that did not liquefy ($r_{u,max}$ = 0.82) in Model 2, a target volumetric strain of 1 percent was used based on the interpretation of strain distribution discussed earlier. Settlement model parameter n was calculated by iteration for each element in the model with the resulting values ranging from 1.72 to 20.0[1].

The numerical modeling was performed in a series of steps. First, the initial non-liquefied soil parameters were assigned and the model was cycled to equilibrium. Two substeps were used, one with elastic parameters and then one with the elasto-plastic Mohr-Coulomb parameters. Next the excess porewater pressures were assigned according to the $r_{u,max}$ profile. This was done incrementally with equilibrium established at each increment to prevent "shocks" to the system from large jumps in porewater pressure. During this stage porewater pressures were fixed in all elements so that drainage would not occur. After the $r_{u,max}$ field was established, the ground surface porewater pressure was fixed at zero and the porewater pressure fixities for the rest of the elements were freed, which allowed groundwater to flow toward the surface and dissipate the excess porewater pressure. During the porewater pressure dissipation phase the elastic moduli were continually updated according to the constitutive laws defined by Equations 1, 2 and 3.

4.3 *Validation results*

For Model 1, the ground surface settlements computed by the numerical model of 0.1 m are in excellent agreement with the centrifuge test results of 0.1 m of surface settlement. This is to be expected since the numerical model parameters were set according to the volumetric strain observed in the experiment. The agreement shows that the proposed constitutive model performs as expected under free field conditions with a uniform soil profile.

In Model 2 the ground surface settlement computed at the center point between columns (node 'A' in Figure 3) was 0.065 m, which is in good agreement with the value of "about 0.07 m" reported by Adalier et al. (2003) for an equivalent location. Figure 4 presents simulation

1. In the upper most 0.4 m the value of n had to be limited to 20 to prevent non-convergence when solving for n. However, limiting n to 20 resulted in negligible error in the calculated free field volumetric settlement.

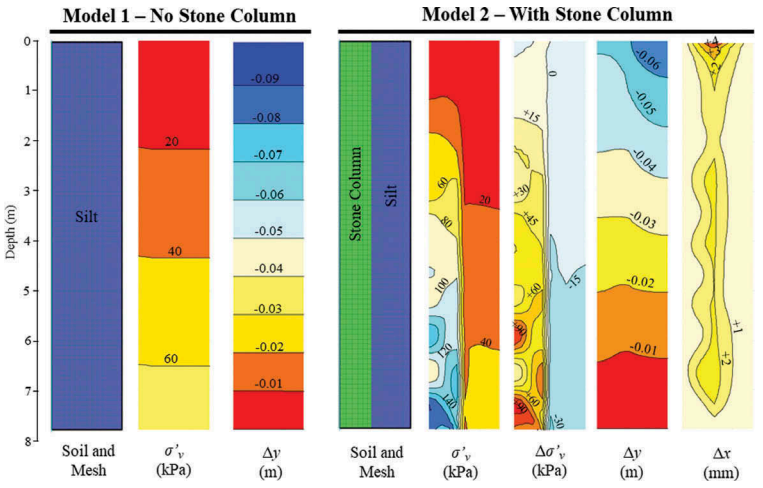

Figure 4. Numerical model stresses and displacements at end of reconsolidation phase

results for Model 1 and Model 2 after the excess porewater pressure has been dissipated. The Model 1 results show an even distribution of vertical stresses and settlement contours (Δy) with depth. As expected, the horizontal displacements (Δx) in Model 1 were essentially zero (results not shown in Figure 4 since they are trivial).

The Model 2 results in Figure 4 include the distribution of vertical stresses (σ'_v) and the change in vertical stresses that occurs between the initial stress conditions before liquefaction and after the dissipation of excess porewater pressures. These results show that the mechanism for reduction of settlements is by shedding of load from the liquefiable silt to the much stiffer stone column. The settlement contours from Model 2 show greater settlement of the silt relative to the stone column in upper half of the model, which is indicative of a downdrag-like mechanism that sheds load from the silt onto the stone column. There are slight positive horizontal displacements for Model 2, which is predominantly a Poisson's effect of the stone column bulging under increased vertical loading. Unfortunately the Adalier et al. (2003) experiments did not include measurements that could be used to validate the computed stress and displacement distributions, but the results seem reasonable.

5 DISCUSSION AND CONCLUSIONS

A constitutive model for post-liquefaction reconsolidation settlement analyses has been developed in this study. The model is a variant of the Mohr-Column elastic perfectly plastic model in FLAC, wherein the elastic moduli vary nonlinearly with effective stress during reconsolidation so that a target volumetric strain is achieved.

The proposed model is convenient and efficient for studies focused on post-liquefaction reconsolidation effects since it avoids the need to use a more advanced constitutive model in a dynamic analysis to generate excess porewater pressures and liquefaction. Instead, excess porewater pressures and volumetric strains are simply specified by the user to represent a desired liquefaction condition. This condition can be determined using simplified methods for liquefaction triggering (e.g., Boulanger and Idriss 2015) and settlements (e.g., Ishihara and Yoshimini 1992).

The proposed constitutive model was validated against two centrifuge tests; one with a uniform silt material (Model 1) and one with the same silt reinforced by an array of stone columns (Model 2). The computed settlement was in excellent agreement with centrifuge Model 1 results indicating that the proposed model is effective at representing reconsolidation settlements under free field conditions. Good agreement was achieved between computed and observed settlement

in the Model 2 case, suggesting that the proposed model is reasonable for use in evaluating reinforcing effects of columnar arrays of ground improvement where post-liquefaction reconsolidation settlement occurs. The model shows the mechanism of settlement reduction is by a downdrag-like shedding of load from the settling silt to the stiffer stone column.

These analyses were performed using an axisymmetric model with no surface loading. They do not account for shear-related building or footing settlement, nor ejecta-related settlement. The results are therefore most relevant to conditions with no surface loading or for deeper liquefiable layers that are outside the influence foundation shear stresses.

The model may also be useful in evaluating other types of liquefaction reconsolidation settlement problems, such as differential settlements due to a spatially varying liquefiable soil or pile downdrag. However, additional validation against experimental data is warranted for such cases.

REFERENCES

Beaty M.H. and Byrne P.M. 2011. UBCSAND Constitutive Model: Version 904aR. Documentation Report: UBCSAND Constitutive Model on Itasca UDM Web Site Report No. UCD/CGM-10/01.

Boulanger, R. W., and Idriss, I. M. 2015. CPT-based liquefaction triggering procedure. *Journal of Geotechnical and Geoenvironmental Engineering*, ASCE, 04015065, 10.1061/(ASCE) GT.1943-5606.0001388.

Boulanger, R.W. and Ziotopoulou, K. 2015. PM4Sand (Version 3): Sand Plasticity Model for Earthquake Engineering Applications, Report No. UCD/CGM-15/1, U.C. Davis.

Bullock, Z., Karimi, Z., Dashti, S., Porter, K., Liel, A.B., Franke, K.W. 2018. A physics-informed semi-empirical probabilistic model for the settlement of shallow-founded structures on liquefiable ground, *Géotechnique*, May 2018.

Bray, J.D., Cubrinovski, M., Zupan, J., and Taylor, M. 2014. Liquefaction Effects on Buildings in the Central Business District of Christchurch. *Earthquake Spectra*: February 2014, Vol. 30, No. 1, pp. 85–109.

Bray J.D. and Macedo, J. 2017. 6th Ishihara Lecture: Simplified procedure for estimating liquefaction-induced building settlement, *Soil Dynamics and Earthquake Engineering*, 102(2017), pp 215–231.

Bray, J.D., Macedo, J. and Luque, R. 2017. Key trends in assessing liquefaction-induced building settlement, *Performance Based Design in Earthquake Geotechnical Engineering*, Vancouver, Canada, July 16–19, 2017.

Hausler, E.A. and Sitar, N. 2001. Performance of soil improvement techniques in earthquakes. *Proceedings of the 4th International Conference on Recent Advances in Geotechnical Earthquake Engineering and Soil Dynamics*, Paper No. 10.15

Itasca Consulting Group 2016. Fast Lagrange Analysis of Continua, Version 8.00.

Ishihara, K., and Yoshimine, M. 1992. Evaluation of settlements in sand deposits following liquefaction during earthquakes, *Soils and Foundations* 32(1),173–188.

Kirsch, K. and Kirsch, F. 2010. *Ground improvement by deep vibratory methods*. London/New York: Spon Press.

Mitchell, J.K., Cooke, H.G., Shaeffer, J.A. 1998. Design considerations in ground improvement for seismic risk mitigation. *Proceedings Geotechnical Earthquake Engineering and Soil Dynamics III*, ASCE GSP No. 75. Seattle, Washington, August 3–6.

Khosravifar, A., Elgamal, A., Lu, J. and Li, J. 2018. A 3D model for earthquake-induced liquefaction triggering and post-liquefaction response, *Soil Dynamics and Earthquake Engineering*, 110(2018) pp 43–52.

Priebe, H.J. 1995. The design of vibro replacement. *Ground Engineering*. 72(3):183–191.

Rayamajhi, D., Ashford, S.A., Boulanger, R.W., Elgamal, A. 2016. Dense granular columns in liquefiable ground. I; Shear reinforcement and cyclic stress ratio reduction, *J. of Geotechnical and Geoenvironmental Engrg*. 04016024, 10.1061/(ASCE)GT.1943-5606.000147.

Sehn, A.L. and Blackburn, J.T. 2008. Predicting performance of aggregate piers. *23rd Central Pennsyvlania Geotechnical Conference*. May 28–30. Hershey, Pennsylvania.

Tokimatsu, K., and Seed, H. B. 1987. Evaluation of settlements in sands due to earthquake shaking, *J. Geotechnical Eng*., ASCE 113(GT8), 861–878.

Ziopotoulou, K. and Boulanger, R.W. 2013. Numerical modeling issues in predicting post-liquefaction reconsolidation strains and settlements, *10th Int. Conf. on Urban Earthquake Engineering, March 1–2,2013*, *Tokyo Institute of Technology*, *Tokyo, Japan*.